Lifetimes of some $2s^2 2p\ ^2P_{3/2}$ states from variational theory

Charlotte Froese Fischer*
National Institute of Standards and Technology, Gaithersburg, Maryland 20899, USA

Ian P. Grant
Mathematical Institute, University of Oxford, Andrew Wiles Building, Radcliffe Observatory Quarter, Woodstock Road, Oxford OX2 6GG, United Kingdom
and Department of Applied Mathematics and Theoretical Physics, University of Cambridge, Wilberforce Road, Cambridge CB3 0WA, United Kingdom

Gediminas Gaigalas and Pavel Rynkun
Institute of Theoretical Physics and Astronomy, Vilnius University, A. Goštauto 12, LT-01108 Vilnius, Lithuania
(Received 11 December 2015; published 5 February 2016)

A measured lifetime of exceptional accuracy has been reported for the $2p\ ^2P_{3/2}$ state of Ar^{13+} that is in good agreement with theory, neglecting the effect of the anomalous magnetic moment. When perturbation theory is used to estimate the effect of the latter, the discrepancy increases. In this paper, results from a fully relativistic variational calculation are presented. By using the Gordon transformation, an expression is derived for the transition matrix element. Lifetimes without and with the effect of the anomalous magnetic moment are reported, both in excellent agreement with perturbation theory.

DOI: 10.1103/PhysRevA.93.022505

I. INTRODUCTION

In nonrelativistic theory the line strength for a magnetic dipole ($M1$) transition between fine-structure levels of a configuration is independent of the wave function. Thus theoretical predictions of lifetimes based on transition rates computed using observed wavelengths are all in remarkable agreement. This was the case for the decay of the $3d\ ^2D_{5/2}$ metastable state of Kr^{17+} [1] where, for seven theoretical lifetimes, all are in the narrow range of 23.83–24.16 ms. Two experimental lifetimes are available, both obtained from electron beam ion trap (EBIT) measurements. The lifetime with the smaller error bar, namely, 24.48 ± 0.32 ms measured by Guise *et al.* [1], is slightly longer than the theory predictions, whereas the measurement with a larger uncertainty, namely, 22.7 ± 1.0 ms reported by Träbert *et al.* [2], is significantly shorter. A comparable situation is observed in a table of the paper by Tupitsyn *et al.* [3] for the decay of the $2p\ ^2P_{3/2}$ state in Ar^{13+} and neighboring members of the isoelectronic sequence. In their paper, the theoretical lifetimes have not been rescaled for observed wavelengths, so a slightly larger variation is shown (about 2%), but this is still much smaller than the variation in experiment which ranges from 8.7(5) to 9.70(15) ms or 11%. The Heidelberg EBIT lifetime measurement of 9.573(4)(5) (stat/syst) ms for the $2p\ ^2P_{3/2}$ state of Ar^{13+} is among the most accurate, if not the most accurate, lifetime measurement ever reported [4,5] and is in excellent agreement with theory when the effect of the anomalous magnetic moment (AMM) of the electron is ignored. Their simple estimate of the effect is 0.46%, an effect much larger that the experimental uncertainty of this measurement. This observation has spurred some in-depth investigations.

Artemyev *et al.* [6] have performed an *ab initio* study of the $2s^2 2p\ ^2P_{1/2}$-$^2P_{3/2}$ transition energy for the argon ion, using perturbation theory and rigorous QED calculations for capturing electron-correlation and the Breit corrections to several orders. Their final value for the transition energy was 22 656.1(3.6) cm^{-1}, in essentially exact agreement with the value of 22 656.239 cm^{-1} derived from observation [7]. This value had also been reported in the Tupitsyn *et al.* [3] paper where additional transition energies were reported for neighboring ions: For K^{14+} the error in the transition energy is somewhat larger, namely, 11 cm^{-1}.

The paper by Tupitsyn *et al.* [3] on the lifetime of the $2s^2 2p\ ^2P_{3/2}$ state of Ar^{13+} is a separate calculation combining several methods. Elaborate calculations are performed in the no-pair Hamiltonian to determine a many-electron wave function where expansion coefficients are used to compute the transition rate using the line strength operator

$$\mathbf{O} = \mathbf{L} + g_s \mathbf{S}, \tag{1}$$

where $g_s = 2$ in relativistic theory but $g_s = 2(1 + a_e)$ when AMM corrections are included. Here, $a_e = 0.001\,159\,652\,180\,73(28)$ is the AMM correction known to high accuracy and whose QED prediction agrees with experiment [8] to the accuracy shown. Contributions are determined from the negative-energy continuum, the higher-order interelectronic corrections, and the AMM effect on the $M1$ transition amplitude by correcting for the anomalous magnetic moment of a free electron. The final predicted lifetime for Ar^{13+} was 9.582 ms without the AMM correction and 9.538(2) ms with the correction. Thus, experiment is in better agreement with theory without than with the correction.

*Charlotte.Fischer@nist.gov

Recently, a number of studies have been reported for the boronlike sequence not included in the earlier study. Energy levels, lifetimes, and $E1$, $M1$, $E2$, and $M2$ transitions of B-like ($Z = 7-30$) ions have been reported by Rynkun *et al.* [9] using multiconfiguration Dirac-Hartree-Fock (MCDHF) and relativistic configuration-interaction (RCI) methods. Marques *et al.* [10] calculated the fine-structure energy splitting of $2s^2 2p\ ^2P$ levels and lifetimes of the $^2P_{3/2}$ level in the boron isoelectronic sequence for $Z = 14-36$, 54, 64, 79, 83, and 92 using the Dirac-Fock multiconfiguration method with both quantum-electrodynamic and electronic correlation corrections. Neither considered the QED correction.

In this paper we analyze results from relativistic variational methods in which a wave function is determined for the initial and final state from which the transition rate is determined in terms of an $M1$ transition matrix element and the transition energy. An expression for the transition operator is derived from first principles that takes into account radiative corrections in the relativistic theory of photon emission and absorption. The line strength is derived from the transition probability. This relativistic expression for $M1$ transitions as derived by Grant [11,12] does not include a g_s factor. Using the Gordon form of the charge-current vector, a different expression has been derived in which the effective magnetic 2^k-pole operator is split into three parts and the anomalous magnetic moment can be introduced in order to capture the AMM effect on the lifetime. A detailed comparison will be made of the differences along the isoelectronic sequence of the line strength derived from the two expressions as well as with other theory. All present calculations were performed using the general relativistic atomic structure package GRASP2K [13,14].

II. RELATIVISTIC THEORY OF MAGNETIC DIPOLE TRANSITIONS

The transition rate for the emission of a single photon from an upper state u to a lower state l is given by [[11], Sec. 4]

$$A_{u\to l} = 2\pi |\langle \Psi_u | \mathcal{H} | \Psi_l \rangle|^2, \quad \mathcal{H} = j^\mu(x) a_\mu(x), \tag{2}$$

where $\mathcal{H}$ is the Hamiltonian describing the interaction between the atomic electron charge-current vector $j^\mu(x)$ and the radiation field 4-potential $a_\mu(x)$ at the space-time point $x = (ct, \boldsymbol{x})$. Summation over pairs of space-time components $\mu = 0,1,2,3$ is implied. Ψ_u and Ψ_l are wave functions for the initial upper u and final lower l states, respectively. Each Ψ is an atomic state function (ASF) of the form

$$\Psi(\Gamma; \pi J) = \sum_j a_j \Phi(\gamma_j; \pi J), \tag{3}$$

where Γ is a label for the state, π its parity, and J its total angular momentum. Φ is an antisymmetric, coupled configuration state function (CSF) of parity π and total angular momentum J. Here, γ specifies the configuration and other quantum numbers that uniquely designate the CSF.

CSFs are constructed from antisymmetrized products of one-electron Dirac 4-component spinors with the general form (in spherical polar coordinates)

$$\psi_{n\kappa m}(x) = \frac{1}{r}\begin{pmatrix} P_{n\kappa m}(r)\chi_{\kappa m}(\theta,\varphi) \\ i\,Q_{n\kappa m}(r)\chi_{-\kappa m}(\theta,\varphi)\end{pmatrix} e^{-iEt}, \tag{4}$$

where n characterizes the orbital energy, and E the total energy of the state. The two component spherical spinors $\chi_{\kappa m}(\theta,\varphi)$ couple the spherical harmonic functions $Y_{lm_l}(\theta,\varphi)$ and the spin function. For "positive-energy" states, $P_{n\kappa}(r)$ and $Q_{n\kappa}(r)$ are referred to as large and small components, respectively.

The interaction $\mathcal{H}$ of the electrons with the radiation field can be expressed in terms of irreducible tensor operators $\boldsymbol{T}$ acting on the coordinates of each active electron. Their symmetry properties ensure that each such irreducible tensor operator can be treated independently. In the case of the magnetic dipole,

$$\begin{aligned} \boldsymbol{T}^{M1}(\boldsymbol{x_i},\omega) &= -ec\boldsymbol{\alpha}\cdot\boldsymbol{A}(\boldsymbol{x_i},\omega), \\ c\boldsymbol{A}(\boldsymbol{x_i},\omega) &= 3i[\boldsymbol{e}\times\boldsymbol{x_i}/r_i]^1 j_1(\omega r_i/c), \end{aligned} \tag{5}$$

where $\boldsymbol{A}(\boldsymbol{x_i},\omega)$ is the $M1$ vector potential acting on the ith electron, $\omega = E_u - E_l > 0$ is the photon energy, $-ec\boldsymbol{\alpha}$ the Dirac matrix operator representing the spacelike part of the electron current, $\boldsymbol{e}$ denotes the photon polarization vector, and $j_1(\omega r_i/c)$ is a spherical Bessel function of order 1. Then it can be shown that [11,12]

$$A^{M1}_{u\to l} = \frac{2\omega}{c}|\langle\Psi(\Gamma_u;\pi_u J_u)\|\mathbf{T}^{M1}\|\Psi(\Gamma_l;\pi_l J_l)\rangle|^2/g_u, \tag{6}$$

where $g_u = 2J_u + 1$. In the case of one-electron transitions, $\alpha \to \beta$ (as for the ground configuration of boronlike systems) [[11], Sec. 4],

$$\begin{aligned} &\langle\alpha\|\boldsymbol{T}^{M1}\|\beta\rangle \\ &= \frac{3}{c\sqrt{2}}(-1)^{j_\alpha+1/2} \\ &\quad\times[(2j_\alpha+1)(2j_\beta+1)]^{1/2}\begin{pmatrix} j_\alpha & 1 & j_\beta \\ 1/2 & 0 & -1/2\end{pmatrix}(\kappa_\alpha+\kappa_\beta) \\ &\quad\times\int_0^\infty\{P^*_\alpha(r)Q_\beta(r)+Q^*_\alpha(r)P_\beta(r)\}j_1(\omega r/c)dr. \end{aligned} \tag{7}$$

Because of the presence of the spherical Bessel function in the integrand, the square of the transition amplitude is energy dependent. Using the usual definition for an $M1$ transition in terms of the line strength S, namely,

$$A^{M1}_{u\to l} = \frac{4}{3}\left(\frac{\omega}{c}\right)^3\frac{S^{M1}_{u\to l}}{g_u},$$

it follows that

$$S^{M1}_{u\to l} = \frac{3}{2}\left(\frac{c}{\omega}\right)^2|\langle u\|\mathbf{T}^{M1}\|l\rangle|^2. \tag{8}$$

The standard form of the relativistic charge-current density, $j^\mu = -ec\bar{\psi}\gamma^\mu\psi$, on which (5) is based provides no obvious way to include the AMM correction. However, Gordon's decomposition [see Ref. [15] and Eq. (2-54) in Ref. [16]) separates the orbital and spin charge currents, replacing (5) by

$$\boldsymbol{T}^{G,M1} = \boldsymbol{T}^{C,1} + g_s(\boldsymbol{T}^{E,1} + \boldsymbol{T}^{B,1}), \tag{9}$$

where $g_s = 2$ is the Dirac g factor. The first term represents the interaction of the orbital motion of a structureless electron with

the photon magnetic field, and the others the interaction of the electron spin with the photon's electric and magnetic fields, respectively. The full relativistic 1-electron reduced matrix elements are

$$\langle\alpha\|\boldsymbol{T}^{C,1}\|\beta\rangle = -\frac{3}{2\sqrt{2}c}\left\{(\kappa_\alpha\|\boldsymbol{l}\|\kappa_\beta)\int_0^\infty P^*_\alpha(r)P_\beta(r)\frac{1}{r}j_1(\omega r/c)dr - (-\kappa_\alpha\|\boldsymbol{l}\|-\kappa_\beta)\int_0^\infty Q^*_\alpha(r)Q_\beta(r)\frac{1}{r}j_1(\omega r/c)dr\right\}, \quad (10)$$

$$\langle\alpha\|\boldsymbol{T}^{E,1}\|\beta\rangle = -\frac{3\omega}{2c^2}\left\{(\kappa_\alpha\|\boldsymbol{C}^1\otimes\boldsymbol{s}\|-\kappa_\beta)\int_0^\infty P^*_\alpha(r)Q_\beta(r)j_1(\omega r/c)dr + (-\kappa_\alpha\|\boldsymbol{C}^1\otimes\boldsymbol{s}\|\kappa_\beta)\int_0^\infty Q^*_\alpha(r)P_\beta(r)j_1(\omega r/c)dr\right\}, \quad (11)$$

$$\langle\alpha\|\boldsymbol{T}^{B,1}\|\beta\rangle = \frac{\omega}{2\,c^2}\left\{\sqrt{2}\left[(\kappa_\alpha\|\boldsymbol{s}\|\kappa_\beta)\int_0^\infty P^*_\alpha(r)P_\beta(r)j_0(\omega r/c)dr - (-\kappa_\alpha\|\boldsymbol{s}\|-\kappa_\beta)\int_0^\infty Q^*_\alpha(r)Q_\beta(r)j_0(\omega r/c)dr\right]\right.$$
$$\left. + \sqrt{5}\left[(\kappa_\alpha\|\boldsymbol{C}^2\otimes\boldsymbol{s}\|\kappa_\beta)\int_0^\infty P^*_\alpha(r)P_\beta(r)j_2(\omega r/c)dr - (-\kappa_\alpha\|\boldsymbol{C}^2\otimes\boldsymbol{s}\|-\kappa_\beta)\int_0^\infty Q^*_\alpha(r)Q_\beta(r)j_2(\omega r/c)dr\right]\right\}, \quad (12)$$

where $\boldsymbol{C}^k$ is the irreducible tensor operator with components $C_{kq}(\theta,\varphi) = [4\pi/(2k+1)]^{1/2}Y^q_k(\theta,\varphi)$. In practice, ω/c is usually a small number, so that all these expressions are dominated by the lowest power of ω/c in a power-series expansion.

In the Pauli approximation, the relative magnitude of small components is $O(1/c)$. So, in the case of the $2s^2 2p\ ^2P^o_{3/2}$-$2s^2 2p\ ^2P^o_{1/2}$ transition in Ar^{13+}, when terms of order $O(1/c^2)$ are omitted, the expressions simplify considerably. For the standard method, as implemented in GRASP,

$$\langle 2p_-\|\boldsymbol{T}^{M1}\|2p_+\rangle \approx \sqrt{6}\int_0^\infty \left[P^*_{2p_-}(r)Q_{2p_+}(r) + Q^*_{2p_-}(r)P_{2p_+}(r)\right]j_1(\omega r/c)dr, \quad (13)$$

whereas, in the Gordon form, the reduced matrix element for the convection current interaction is

$$\langle 2p_-\|\boldsymbol{T}^{C,1}\|2p_+\rangle \approx \frac{\sqrt{6}}{c}\int_0^\infty P^*_{2p_-}(r)P_{2p_+}(r)j_1(\omega r/c)\frac{dr}{r}, \quad (14)$$

$\langle 2p_-\|\boldsymbol{T}^{E,1}\|2p_+\rangle$ is negligible, and the matrix element for the spin B-field interaction is

$$\langle 2p_-\|\boldsymbol{T}^{B,1}\|2p_+\rangle \approx -\sqrt{\frac{2}{3}}\frac{\omega}{c^2}\left\{\int_0^\infty P^*_{2p_-}(r)P_{2p_+}(r)j_0(\omega r/c)dr + \frac{1}{4}\int_0^\infty P^*_{2p_-}(r)P_{2p_+}(r)\ j_2(\omega r/c)dr\right\}. \quad (15)$$

The transition matrix element of Eq. (9) can now be evaluated with $g_s = 2$ in the standard Dirac form or with $g_s = 2(1+a_e)$ in order to include the AMM correction. Notice that, unlike the standard form [Eq. (13)] where the radial integral depends equally on the large and small components of the orbitals entering into the transition, in the Gordon form, all the significant radial integrals are expressed in terms of the large component alone. Since $j_0(\omega r/c) = 1 + O(\omega r/c)^2$ and $j_1(\omega r/c)/r = (\omega r/3c)\,[1 + O(\omega r/c)^2]$, the leading terms of both (14) and (15) are of the same order $O(\omega/c^2)$, so that $S^{M1}_{u\to l}$ [Eq. (8)] is of order $O(1/c^2)$ and is roughly independent of ω.

III. GRASP2K CALCULATIONS FOR THE $2s^2 2p\ ^2P_{1/2,3/2}$ STATES OF Ar^{13+}

Systematic variational calculations using the multiconfiguration Dirac-Hartree-Fock method have been published for selected elements of the boronlike sequence by Rynkun *et al.* [9]. Briefly, starting with the multireference (MR) set of CSFs, $2s^2 2p$ and $2p^3$, for $J = 1/2$ and $J = 3/2$, wave-function expansions over a basis of configuration state functions were obtained through single (S) and double (D) substitutions to orbitals in an active set, characterized by the maximum principal quantum number n and the maximum orbital angular quantum number $l \leqslant 6$. Thereafter, the maximum value of l decreased. For $n = 8$, l was limited to $l \leqslant 5$, whereas for $n = 9$, the limit was $l \leqslant 4$. These calculations were performed using the Dirac-Coulomb Hamiltonian and a Fermi model for the nuclear potential. In a separate configuration interaction calculation the frequency-dependent Breit, vacuum polarization (VP), and self-energy (SE) matrix elements were added to the Hamiltonian matrix. The wave functions from the latter were then used to determine the transition rate.

One of the factors affecting the accuracy of the transition rate in a variational procedure is the accuracy of the transition energy [17,18]. Unlike the earlier study [9], where all the levels of a selected spectrum and all allowed transitions between them were reported, in this work only the $M1$ transition is of concern. Also, in view of the recent publication by Artemyev *et al.* [6] who break down the contributions to the total energy from different corrections, it is possible to evaluate the reliability of the way in which corrections are included in the GRASP2K computational procedure, particularly with respect to Breit and QED corrections.

Table I shows the convergence of the individual total energies (in E_h), the transition energy in cm^{-1}, as well as both *ab initio* (ai) and scaled (adj) transition rates for the three formulas, scaled so that the transition rate corresponds to the rate obtained when the observed transition energy is used with a given line strength. Though the total energies are systematically decreasing (as required by theory), the energy difference for calculations up to $n = 9$ have been a

TABLE I. Total energies (E_h), transition energies $\Delta E = \omega$ (cm^{-1}) and transition rates A (s^{-1}) of $M1$ transition $2s^2 2p\,{}^2P^o_{3/2}$-$2s^2 2p\,{}^2P^o_{1/2}$ for boronlike Ar^{13+} from RCI calculations including Breit and QED corrections. Reported are *ab initio* (ai) and adjusted (adj) transition rates. The latter were obtained by scaling the computed transition rates by r^3 where $r = \Delta E_{\rm observed}/\Delta E_{\rm computed}$. Results in lines with "MR" are those from calculations with an enlarged MR set.

				A (Standard)		A (Gordon)		A (Gordon_AMM)	
n	$E(^2P^o_{1/2})$	$E(^2P^o_{3/2})$	ΔE	ai	adj	ai	adj	ai	adj
MR	−406.9250935	−406.8219645	22 634.21	104.076	104.380	104.081	104.385	104.564	104.870
3	−407.0061715	−406.9030321	22 636.49	104.107	104.380	104.116	104.389	104.599	104.873
4	−407.0288719	−406.9256172	22 661.79	104.455	104.378	104.457	104.380	104.943	104.866
5	−407.0386858	−406.9354266	22 662.78	104.472	104.382	104.470	104.380	104.956	104.865
6	−407.0434877	−406.9401939	22 670.37	104.573	104.378	104.575	104.380	105.061	104.865
7	−407.0457974	−406.9425121	22 668.50	104.546	104.376	104.549	104.379	105.035	104.865
8	−407.0469090	−406.9436277	22 667.62	104.533	104.376	104.537	104.380	105.022	104.864
9	−407.0474503	−406.9441684	22 667.75	104.536	104.377	104.539	104.380	105.024	104.864
9_MR	−407.0475470	−406.9442626	22 668.29	104.543	104.376	104.546	104.379	105.032	104.865
10_MR	−407.0478115	−406.9445273	22 668.25	104.542	104.376	104.546	104.380	105.031	104.864
Other theory									
Cheng [19]			22 795						
Galavis [20]			22 362						
Dong [21]			22 636						
Artemyev *et al.* [6]			22 656.1(3.6)						
Observed									
NIST [7]			22 656.239						

bit irregular, although it has decreased by only 0.75 cm^{-1} in going from $n = 7$ to $n = 9$. The effect on this trend of restricting the l-quantum number when $n > 7$ was found to be negligible (0.2 cm^{-1}). At the final stage the multireference sets for the states of the $2s^2 2p$ and $2p^3$ configurations were enlarged to include $\{2s^2 2p, 2p^3, 2s2p3d, 2p3d^2\}$ in order to estimate the uncertainty in our result. This multireference was chosen based on the criteria that it should contain the configurations that had the largest weights in the preceding self-consistent field calculations. Among the states generated by single-double (SD) excitations from the multireference set, only those interacting with at least one member of the set were retained. The effect of restricting the MR set is the difference between the $n = 9$_MR value shown in the table and the $n = 9$ energy or an increase of 0.54 cm^{-1}.

Also included in this table are some of the more accurate transition energies from other theories. The Dong [21] value agrees exactly with the present $n = 3$ results. All theories are compared with the critically evaluated NIST value [7]. The systematic computed energies have converged to a value of 22 667.75 cm^{-1} with an estimated error of 0.5 cm^{-1} in the Dirac-Coulomb approximation (difference between the 10_MR and $n = 9$ transition energies). Adjusted transition rates have converged to at least four significant digits.

It is important to see how the present method has included various corrections to the Dirac-Coulomb Hamiltonian, a procedure that differs from what is adopted in perturbation theory methods [3,6]. For each n, variational calculations are performed for the Dirac-Coulomb Hamiltonian,

$$H_{\rm DC} = \sum_{i=1}^{N} \left[c\boldsymbol{\alpha}_i \cdot \boldsymbol{p}_i + (\beta_i - 1)c^2 + V_i^N \right] + \sum_{i>j}^{N} \frac{1}{r_{ij}}, \quad (16)$$

where V^N is the monopole part of the electron-nucleus Coulomb interaction, $\boldsymbol{\alpha}$ and β the 4×4 Dirac matrices, and c the speed of light in atomic units. These calculations optimized the large (P) and small (Q) radial factors of the one-electron orbitals. This was followed by a CI calculation for the Dirac-Coulomb-Breit Hamiltonian $H_{\rm DCB} = H_{\rm DC} + H_{\rm Breit}$, where

$$H_{\rm Breit} = -\sum_{i<j}^{N} \left[\boldsymbol{\alpha}_i \cdot \boldsymbol{\alpha}_j \frac{\cos(\omega_{ij} r_{ij}/c)}{r_{ij}} + (\boldsymbol{\alpha}_i \cdot \boldsymbol{\nabla}_i)(\boldsymbol{\alpha}_j \cdot \boldsymbol{\nabla}_j) \frac{\cos(\omega_{ij} r_{ij}/c) - 1}{\omega_{ij}^2 r_{ij}/c^2} \right] \quad (17)$$

is the transverse photon interaction.

Next, the matrix element for vacuum polarization, $H_{\rm VP}$, is added to the diagonal matrix elements,

$$\langle \gamma J | H_{\rm VP} | \gamma' J \rangle = \sum_{a=1}^{n_w} w_a \int_0^\infty V_{\rm VP}(r) u_a^\dagger(r) u_a(r) dr, \quad (18)$$

where u_a is the radial spinor, $u_a^\dagger$ is the Hermitian conjugate of u_a, and $V_{\rm VP}(r)$ includes vacuum polarization potentials of both second and fourth order in QED perturbation theory.

Finally, the self-energy contributions $H_{\rm SE}$ based on a screened hydrogenic method are added to the diagonal matrix elements for each orbital of the CSF, namely,

$$\langle \gamma J | H_{\rm SE} | \gamma' J \rangle = \sum_{a=1}^{n_w} w_a E_{\rm SE}(a), \quad (19)$$

where n_w is the number of subshells in the CSF, w_a is the number of electrons in subshell a in CSF, and $E_{\rm SE}(a)$ is the one-electron self-energy of an electron in subshell a.

TABLE II. Contributions to the total energies of $2s^2 2p\ ^2P^o_{1/2}$ and $2s^2 2p\ ^2P^o_{3/2}$ states, and their transition energies in B-like Ar^{13+} from variational calculations as a function of the orbital set. All results are in cm^{-1}. See text for how various corrections were determined.

$n =$	DHF	3	4	5	6	7	8	9
				Total energy of $2s^2 2p\ ^2P^o_{1/2}$				
DHF	−89324562.486	−89324562.486	−89324562.486	−89324562.486	−89324562.486	−89324562.486	−89324562.486	−89324562.486
Correl.		−42855.350	−47767.407	−49779.380	−50717.992	−51151.944	−51343.792	−51418.613
Breit	21500.231	20641.692	20569.411	20425.551	20312.562	20239.582	20187.362	20143.399
VP	−1468.072	−1464.093	−1463.722	−1463.458	−1463.551	−1463.626	−1463.608	−1463.617
SE	20783.034	20711.056	20712.873	20714.537	20712.328	20712.426	20712.505	20712.491
Total	−89283747.293	−89327529.182	−89332511.330	−89334665.236	−89335719.140	−89336226.048	−89336470.019	−89336588.826
				Total energy of $2s^2 2p\ ^2P^o_{3/2}$				
DHF	−89300172.520	−89300172.520	−89300172.520	−89300172.520	−89300172.520	−89300172.520	−89300172.520	−89300172.520
Correl.	−43522.425	−48406.183	−50423.166	−51363.317	−51799.249	−51992.495	−52067.318	
Breit	20300.533	19508.325	19432.552	19288.684	19177.247	19103.796	19051.974	19008.078
VP	−1467.875	−1463.827	−1463.472	−1463.198	−1463.294	−1463.370	−1463.352	−1463.359
SE	20835.230	20757.757	20760.084	20767.745	20773.116	20773.790	20773.997	20774.045
Total	−89260504.632	−89304892.690	−89309849.539	−89312002.456	−89313048.767	−89313557.552	−89313802.396	−89313921.074
				Transition energy				
DHF	24389.967	24389.967	24389.967	24389.967	24389.967	24389.967	24389.967	24389.967
Correl.	−667.075	−638.777	−643.786	−645.326	−647.306	−648.704	−648.705	
Breit	−1199.698	−1133.367	−1136.859	−1136.867	−1135.314	−1135.785	−1135.388	−1135.321
VP	0.197	0.266	0.249	0.260	0.257	0.256	0.256	0.257
SE	52.195	46.700	47.210	53.208	60.788	61.364	61.492	61.554
Total	23242.661	22636.491	22661.791	22662.781	22670.373	22668.496	22667.623	22667.752

TABLE III. Comparison of contributions to the ground state $2s^2 2p\ ^2P_{1/2}$ total energy (in cm^{-1}) from the present work with that of Marques *et al.* [10].

Contrib.	Present ($n = 9$)	Ref. [10]
DHF+Corr.+VP	−89377444	−89374349
Breit	20143	20406
SE	20712	20720
Total	−89336589	−89333223

As additional operators are included in the Hamiltonian, the difference in the energy defines the contribution from the most recently added operator. The contribution to the energy (eigenvalue) is not totally independent of the order in which corrections are added, but in the present work we assume the above order. Thus a second-order perturbation correction involving both the Coulomb operator and the Breit operator would be a Breit correction in this process. The energy from a H_{DC} calculation defines the correlation correction relative to the Dirac-Hartree-Fock energy for the single $2s^2 2p$ CSF.

Table II shows the convergence of the correlation, Breit, vacuum polarization, and self-energy corrections as a function of n from the above procedure. Also shown is the Dirac-Hartree-Fock energy, the total energy for the $2s^2 2p\ ^2P_{1/2}$ and $2s^2 2p\ ^2P_{3/2}$ states, and the transition energy for each n. From this table it is clear that the correlation, Breit, and vacuum polarization are changing with the wave-function expansion and are interrelated, whereas self-energy is less affected. The correlation and Breit corrections to the total energies of the individual states have not converged, but because core-core effects largely cancel in the transition energy, the different effects have converged for the transition energy.

GRASP2K [13,14] is often compared with results from MCDFGME [22,23]. In Table III the present contributions to the total energy of the $2s^2 2p\ ^2P^o_{1/2}$ ground state are compared with those reported by Marques *et al.* [10] using the MCDFGME code. That correlation was limited in their work is clearly evident from the higher total energy. The Breit correction is similar to the $n = 5$ correction in the present work. In order to include as much of the Breit correction in a single (or a few) configuration calculation in MCDFGME [22,23] as possible, the Breit operator is included in the variational calculation for the orbitals so that, by Brillouin's theorem, certain correlation effects are included implicitly. Since the correlation and the Breit correction interact, and the Breit operator is computationally intensive, for a variational method it is more efficient to include the operator only in the final CI calculation. On the other hand, the SE correction is relatively independent of the Breit and correlation effects and would be expected to be similar for the two methods. Table III shows that the present SE correction is 8 cm^{-1} smaller than the Marques *et al.* value [10].

TABLE IV. Comparison of contributions to the transition energy (in cm^{-1}) in Ar^{13+} from the present work with that of Artemyev *et al.* [6] based on the core-Hartree (CH) potential.

Contrib.	Present work	Ref. [6]
DHF	24389.967	24343.0
Corr.	−648.705	−1002.9
Breit	−1135.321	−728.2
QED	61.811	45.0
Total	22667.752	22656.9

TABLE V. Transition energies $\Delta E = \omega$ (cm^{-1}) and line strength S of $M1$ transition $2s^2 2p\ ^2P^o_{3/2}$-$2s^2 2p\ ^2P^o_{1/2}$ for boronlike Ar from RCI calculations including Breit and QED corrections.

n	ΔE	S (Standard)	S (Gordon)	S (Gordon_AMM)
MR	22 634.21	1.33100	1.33106	1.33724
3	22 636.49	1.33099	1.33110	1.33728
4	22 661.79	1.33097	1.33100	1.33719
5	22 662.78	1.33102	1.33100	1.33718
6	22 670.37	1.33097	1.33099	1.33717
7	22 668.50	1.33095	1.33099	1.33717
8	22 667.62	1.33094	1.33099	1.33717
9	22 667.75	1.33095	1.33099	1.33717

Artemyev *et al.* [6] tabulate contributions to the transition energy for various initial potentials. Results from their core-Hartree potential are compared in Table IV with the present work. Included in the correlation category was the first-order interaction energy. All the second-order or higher-interaction Breit contributions have been included as Breit corrections, and all contributions associated with QED are listed here as the QED correction. Exact agreement is not expected, although the sum of contributions should agree with the observed transition energy. This comparison suggests that the present contributions to the QED correction are somewhat too large in the GRASP2K code. From Table II it is seen that $n = 5$ results are in better agreement than those from $n = 9$ which included more correlation orbitals. With a QED contribution in agreement with the correction obtained by Artemyev, the two calculations would be in excellent agreement. Even the DHF value would improve agreement.

Table V shows the line strength (derived from the transition rates) for the standard GRASP2K [Eq. (7)] and Gordon [Eq. (9) without and with the AMM correction] formulas for energy adjusted transition rates. Clearly evident is that the first two are identical to four decimal places whereas the third has increased by 0.46%. In nonrelativistic theory the line strength for the MR

TABLE VI. Energy adjusted lifetimes τ (ms) of the $2s^2 2p\ ^2P^o_{3/2}$ level for boronlike Ar^{13+} from RCI calculations including Breit and QED corrections.

n	τ (Gordon)	τ (Gordon_AMM)
MR	9.57990	9.53565
3	9.57958	9.53534
4	9.58036	9.53599
5	9.58042	9.53606
6	9.58042	9.53610
7	9.58043	9.53610
8	9.58041	9.53617
9	9.58040	9.53615

set is exactly 4/3. The slight deviation noticed in the table is due to the fact that the orbitals for $2p_{1/2}$ and $2p_{3/2}$ are not exactly the same arising from a relativistic effect. The effect of correlation is small and the line strength has converged to five decimal places by $n = 6$. Because of the similarity of line strengths for standard GRASP2K and Gordon formula, results for the former will not be consider further in the remaining tables.

Table VI shows the convergence of the energy adjusted lifetimes for the Gordon formulas, without and with the AMM correction. The energy adjusted values have converged to at least four decimal places.

IV. THE BORONLIKE SEQUENCE

The analysis described above for Ar^{13+} has been applied to the boronlike sequence. Figure 1 shows that, indeed, the line strengths from the GRASP2K and Gordon expressions are essentially identical and that the AMM correction remains similar for a wide range on Z.

In Table VII the present energy adjusted lifetimes from the Gordon form, without and with the AMM correction, are listed for selected elements of the boronlike sequence. Also listed are some other experimental values. For Ar^{13+}, the other (earlier) lifetimes have much larger uncertainties than the Heidelberg EBIT value. In comparison with the present findings, the Livermore EBIT measurement [25] is on the

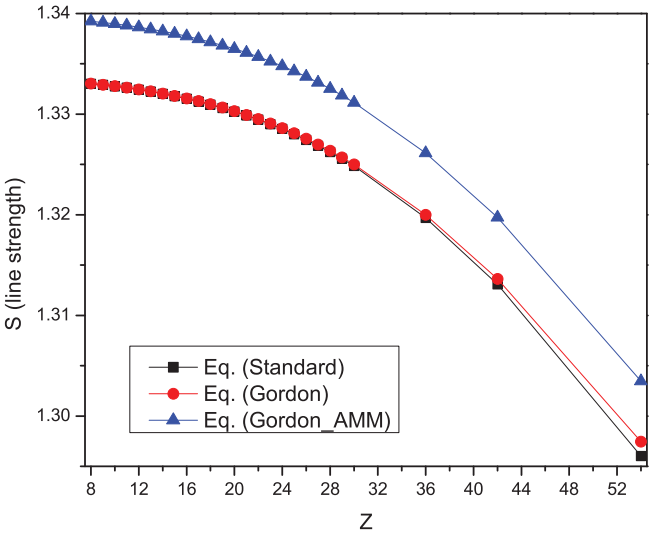

FIG. 1. Line strength (S) dependence on Z for $2s^2 2p\ ^2P^o_{3/2}$-$2s^2 2p\ ^2P^o_{1/2}$ $M1$ transitions for boronlike ions.

TABLE VII. Lifetimes τ (in ms) of the $2s^2 2p\ ^2P^o_{3/2}$ level for boron isoelectronic sequences from RCI calculations including Breit and QED corrections. Reported are the adjusted lifetimes without and with the AMM corrections from the present work. Observed energies were taken from NIST [7]. Experimental lifetimes are followed by uncertainty in ms given in parentheses whereas theoretical lifetimes from [10] have been energy adjusted.

Ion	Z	τ (Gordon)	τ (Gordon_AMM)	τ (Expt.)	τ (Theory [10])
O^{3+}	$Z = 8$	1.9358×10^{6}	1.92687×10^{6}		
F^{4+}	$Z = 9$	2.6960×10^{5}	2.6835×10^{5}		
Ne^{5+}	$Z = 10$	4.9858×10^{4}	4.9628×10^{4}		
Na^{6+}	$Z = 11$	1.1441×10^{4}	1.1388×10^{4}		
Mg^{7+}	$Z = 12$	3.0913×10^{3}	3.0770×10^{3}		
Al^{8+}	$Z = 13$	9.5193×10^{2}	9.4753×10^{2}		
Si^{9+}	$Z = 14$	3.2588×10^{2}	3.2437×10^{2}		3.259×10^{2}
P^{10+}	$Z = 15$	1.2204×10^{2}	1.2147×10^{2}		1.221×10^{2}
S^{11+}	$Z = 16$	4.9141×10^{1}	4.8913×10^{1}		4.915×10^{1}
Cl^{12+}	$Z = 17$	2.1108×10^{1}	2.1011×10^{1}	2.12×10^{1}(0.6) [24]	2.111×10^{1}
				2.11×10^{1}(0.5) [24]	
Ar^{13+}	$Z = 18$	9.5804	9.5361	9.573 (0.006) [4,5]	9.582
		9.582[a]	9.538[a]	9.70 (0.15) [25]	
				9.12 (0.18) [26]	
K^{14+}	$Z = 19$	4.5614	4.5403	4.47 (0.10) [27]	4.563
Ca^{15+}	$Z = 20$	2.2886	2.2781		2.289
Sc^{16+}	$Z = 21$	1.1731	1.1677		1.174
Ti^{17+}	$Z = 22$	6.2704×10^{-1}	6.2414×10^{-1}	6.27×10^{-1}(0.010) [28]	6.273×10^{-1}
V^{18+}	$Z = 23$	3.4547×10^{-1}	3.4387×10^{-1}		3.456×10^{-1}
Cr^{19+}	$Z = 24$	1.9542×10^{-1}	1.9451×10^{-1}		1.955×10^{-1}
Mn^{20+}	$Z = 25$	1.1383×10^{-1}	1.1330×10^{-1}		1.138×10^{-1}
Fe^{21+}	$Z = 26$	6.7529×10^{-2}	6.7217×10^{-2}		6.755×10^{-2}
Co^{22+}	$Z = 27$	4.1352×10^{-2}	4.1161×10^{-2}		4.137×10^{-2}
Ni^{23+}	$Z = 28$	2.5366×10^{-2}	2.5248×10^{-2}		2.537×10^{-2}
Cu^{24+}	$Z = 29$	1.5983×10^{-2}	1.5909×10^{-2}		1.599×10^{-2}
Kr^{31+}	$Z = 36$	9.4009×10^{-4}	9.3575×10^{-4}		9.404×10^{-4}
Mo^{37+}	$Z = 42$	1.2587×10^{-4}	1.2529×10^{-4}		

[a]From Tupitsyn *et al.* [3].

high side, at the edge of their 1σ error range, while the result obtained by Moehs and Church [26] is low, beyond their 1σ error. The experimental uncertainties for the measurements for Cl^{12+} [24], K^{14+}[27], and Ti^{17+} [28] each encompass both theoretical results, with and without AMM corrections, and cannot discriminate between the two. The *ab initio* lifetimes reported by Marques *et al.* [10] have been adjusted to observed wavelengths in this table and are in good agreement with the present lifetimes without the AMM correction.

V. CONCLUSIONS

In this paper, the lifetime of the $2s^2 2p\ ^2P_{3/2}$ level of Ar^{13+} has been investigated in detail using a fully relativistic variational method. The accuracy of the resulting wave function defines the accuracy of the line strength and hence that of the lifetime when the observed wavelength is used for computing the transition probability. Our results of [9.5804(16) ms, 9.5361(16) ms] for the lifetime, without and with the AMM correction, respectively, is in excellent agreement with the [9.582(2) ms, 9.538(2) ms] values reported by Tupitsyn *et al.* [3]. These values need to be compared with the most accurate measurement by Lapierre *et al.* [4]. Including the QED correction in the transition operator increases the line strength and hence lowers the lifetime. Stone [29], in his paper deriving the expression for the Breit interaction, includes a g_s factor for some contributions. For consistency, this AMM effect on the Breit operator should also be included, but a preliminary investigation showed that the effect on the line strength is negligible. The experimental value is in better agreement with the higher value of the lifetime without the correction. Thus the source of the discrepancy remains unresolved.

[1] N. D. Guise, J. N. Tan, S. M. Brewer, Ch. F. Fischer, and P. Jönsson, Phys. Rev. A **89**, 040502(R) (2014).

[2] E. Träbert, P. Beiersdorfer, G. V. Brown, H. Chen, D. B. Thorn, and E. Biémont, Phys. Rev. A **64**, 042511 (2001).

[3] I. I. Tupitsyn, A. V. Volotka, D. A. Glazov, V. M. Shabaev, G. Plunien, J. R. Crespo López-Urrutia, A. Lapierre, and J. Ullrich, Phys. Rev. A **72**, 062503 (2005).

[4] A. Lapierre, U. D. Jentschura, J. R. Crespo López-Urrutia, J. Braun, G. Brenner, H. Bruhns, D. Fischer, A. J. Gonzalez Martinez, Z. Harman, W. R. Johnson, C. Keitel, V. Mironov, C. J. Osborne, G. Sikler, R. Soria Orts, V. Shavaev, H. Tawara, I. I. Tupitsyn, J. Ullrich, and A. Volotka, Phys. Rev. Lett. **95**, 183001 (2005).

[5] A. Lapierre, J. R. Crespo López-Urrutia, J. Braun, G. Brenner, H. Bruhns, D. Fischer, A. J. González Martínez, V. Mironov, C. Osborne, G. Sikler, R. Soria Orts, H. Tawara, and J. Ullrich, V. M. Shabaev, I. I. Tupitsyn, and A. Volotka, Phys. Rev. A **73**, 052507 (2006).

[6] A. N. Artemyev, V. M. Shabaev, I. I. Tupitsyn, G. Plunien, and V. A. Yerokhin, Phys. Rev. Lett. **98**, 173004 (2007).

[7] A. E. Kramida, Yu. Ralchenko, J. Reader, and NIST ASD Team (2014), NIST Atomic Spectra Database (ver. 5.2), http://physics.nist.gov/asd (accessed 2015 June 11), National Institute of Standards and Technology, Gaithersburg, MD.

[8] J. Schwinger, Phys. Rev. **73**, 416 (1948).

[9] P. Rynkun, P. Jönsson, G. Gaigalas, C. Froese Fischer, At. Data Nucl. Data Tables **98**, 481 (2012).

[10] J. P. Marques, P. Indelicato, and F. Parente, Eur. Phys. J. D **66**, 324 (2012).

[11] I. P. Grant, J. Phys. B **7**, 1458 (1974); typographical errors in this paper were corrected in *Methods in Computational Chemistry*, edited by S. Wilson (Plenum, New York, 1988), Vol. 2, pp. 1–71.

[12] I. P. Grant, *Relativistic Quantum Theory of Atoms and Molecules: Theory and Computation* (Springer, Berlin, 2006).

[13] P. Jönsson, G. Gaigalas, J. Bieroń, C. Froese Fischer, and I. P. Grant, Comput. Phys. Commun. **184**, 2197 (2013).

[14] P. Jönsson, J. Bieroń, T. Brage, J. Ekman, C. Froese Fischer, G. Gaigalas, M. Godefroid, I. P. Grant, and J. Grumer, *A Practical Guide to GRASP2K*, http://ddwap.mah.se/tsjoek/compas

[15] W. Gordon, Z. Phys. **50**, 630 (1928).

[16] C. Itzykson and J.-B. Zuber, *Quantum Field Theory* (McGraw-Hill, New York, 1980).

[17] C. Froese Fischer, Phys. Scr., T **134**, 014019 (2009).

[18] C. Froese Fischer, J. Phys. B **43**, 074020 (2010).

[19] K.-T. Cheng, Y.-K. Kim, and J. P. Desclaux, At. Data Nucl. Data Tables **24**, 111 (1979).

[20] M. E. Galavis, C. Mendoza, and C. J. Zeippen, Astron. Astrophys. Suppl. **131**, 499 (1998).

[21] C. Z. Dong, S. Fritzsche, B. Fricke, and W.-D. Sepp, Phys. Scr., T **92**, 294 (2001).

[22] J. P. Desclaux, Relativistic Multiconfiguration Dirac-Fock package, in *Methods and Techniques in Computational Chemistry*, edited by E. Clementi (STEF, Cagliari, 1993).

[23] P. Indelicato and J. P. Desclaux, MCDFGME (ver. 2011), a multiconfiguration Dirac-Fock and general matrix elements program, http://dirac.spectro.jussieu.fr/mcdf/

[24] E. Träbert, P. Beiersdorfer, G. Gwinner, E. H. Pinnington, and A. Wolf, Phys. Rev. A **66**, 052507 (2002).

[25] E. Träbert, P. Beiersdorfer, S. B. Utter, G. V. Brown, H. Chen, C. L. Harris, P. A. Neill, D. W. Savin, and A. J. Smith, Astrophys. J. **541**, 506 (2000).

[26] D. P. Moehs and D. A. Church, Phys. Rev. A **58**, 1111 (1998).

[27] E. Träbert, P. Beiersdorfer, G. V. Brown, H. Chen, E. H. Pinnington, and D. B. Thorn, Phys. Rev. A **64**, 034501 (2001).

[28] E. Träbert, G. Gwinner, A. Wolf, X. Tordoir, and A. G. Calamai, Phys. Lett. A **264**, 311 (1999).

[29] A. P. Stone, Proc. Phys. Soc. **77**, 786 (1961).